Potential Use of OCT Imaging in Clinical Practice

From preintervention to postprocedure follow-up, the utility of optical coherence tomography assessment is examined.

BY DANIEL CHAMIÉ, MD, AND RICARDO A. COSTA, MD, PHD

Historically, coronary angiography has been the workhorse invasive imaging tool for coronary diagnostic and invasive procedures. As a luminogram, coronary angiography has intrinsic limitations in cases of vessel foreshortening and overlapping and does not provide information regarding plaque composition and vessel morphology. Intravascular ultrasound (IVUS) provides real-time tomographic cross-sectional images of the coronary vessel wall, allowing for quantification of luminal and vessel dimensions, as well as identification of plaque type, location, distribution, size, and burden.

IVUS has been of fundamental importance in the development of interventional cardiology, providing unique insights into the understanding of coronary atherosclerosis and refinements on percutaneous interventional procedures, being considered the gold standard intravascular imaging method to guide percutaneous coronary interventions (PCI) and investigate vascular responses to coronary stents. However, IVUS has limited axial resolution (100–150 µm),[1] which can affect its ability to detect acute effects of PCI and vascular response to drug-eluting stents (DES).

Intravascular optical coherence tomography (OCT) is a recently developed light-based imaging modality that uses near-infrared light as its energy source. OCT provides cross-sectional tomographic images of the internal vascular environment, with high axial (10–15 µm) and lateral (20–90 µm) resolutions, by measuring the echo time delay and magnitude of backscattered light.[1,2] To date, OCT has been mostly used in the research field, providing new insights into the pathophysiology of atherosclerosis and vascular response to coronary stents. In this article, we discuss the potential clinical applications of OCT.

PREINTERVENTION USE OF OCT

Atherosclerosis Characterization and Plaque Morphology

OCT has proven to be accurate in visualizing all three arterial layers in a normal coronary artery and in detecting even small degrees of intimal thickening. OCT has also demonstrated high sensitivities and specificities for discrimination of different components of atherosclerotic disease, such as fibrotic, fibrocalcific, and lipid-rich plaques.[3-5] It also showed high accuracy and sensitivity in identifying and quantifying different features of the so-called vulnerable plaques prone to rupture, such as lipid content, fibrous cap thickness,[6,7] and macrophage infiltration.[8,9] In comparison to angioscopy and IVUS, OCT demonstrated a superior ability to detect plaque rupture, fibrous cap erosion, and intraluminal thrombus in acute coronary syndrome (ACS) patients.[10] High sensitivity and specificity in differentiating red (erythrocyte-rich) from white (platelet-rich) thrombus has also been demonstrated.[11]

These features make OCT an invaluable imaging tool for in vivo characterization of atherosclerosis and investigation of plaque morphologies (Figure 1), which may provide useful insights into the mechanisms leading to ACS and help to identify vulnerable lesions that might be at high risk of a future adverse event. Furthermore, accurate plaque characterization may aid in deciding the best landing zone for intracoronary stenting and selecting adjunctive devices and therapies, such as rotational atherectomy, thrombectomy, dedicated devices, and medications.

Assessment of Stenosis Severity

OCT provides accurate information regarding lumen dimensions and quantification of target stenosis, which are important in clinical decision making and planning interventional procedures. Due to a very clear interface between the vascular lumen and the intima layer of the vessel, accurate, automated, and reproducible measurements of lumen area have been accomplished with OCT both in vitro and in vivo.[12-14] It is important to note that OCT usually underestimates lumen area in comparison to IVUS measurements.

In an in vivo study, IVUS demonstrated larger lumen areas in comparison to the first-generation time-domain OCT measurements of coregistered vessel segments when OCT images were acquired with a proximal balloon occlusion technique (the lumen area, as determined by IVUS, was 33.7% larger than by OCT). In addition, some preliminary studies suggest this may also be the case with nonocclusive techniques (the lumen area, as determined by IVUS, was 21.5% larger than that determined by time-domain OCT).[15] At this point, such differences between methods have to be taken into account when using previously established IVUS criteria during OCT examination for clinical decision making, but new studies with new-generation OCT systems are currently ongoing to better assess this issue.

A variety of observational studies validated IVUS-derived parameters against invasive and noninvasive tests for the assessment of lesion severity. An absolute minimal lumen area (MLA) < 4 mm^2 correlated strongly with a coronary flow reserve < 2,[16] a fractional flow reserve (FFR) < 0.75,[17] and perfusion defects on single-photon emission computed tomography.[18] In a recent validation study with a total of 236 lesions in 201 patients, an MLA < 2.4 mm^2 was identified as the best cutoff to predict an FFR < 0.8, with a diagnostic accuracy of 68% and a sensitivity of 90%. However, poor specificity (60%) limited the value of the anatomical IVUS MLA cutoff to predict physiological significance of coronary lesions.[19]

More recently, Gonzalo et al[20] assessed the diagnostic efficiency of OCT and IVUS in identifying hemodynamically significant coronary stenosis as determined by FFR. Both OCT and IVUS presented moderate diagnostic accuracy for identifying physiologically significant stenosis. The best cutoff values of OCT-derived measurements to identify stenosis with an FFR ≤ 0.8 were 1.95 mm^2 for MLA (82% sensitivity and 63% specificity) and 1.34 mm for minimal lumen diameter (82% sensitivity and 67% specificity). Optimal cut-off values for IVUS-derived parameters were 2.36 mm^2 for MLA (67% sensitivity and 65% specificity) and 1.59 mm for minimal lumen diameter (67% sensitivity and 65% specificity). This study reinforces the low specificities of intravascular anatomic metrics to predict functionally significant stenosis, precluding the routine use of OCT and IVUS as substitutes for FFR regarding the decision making of intermediate angiographic stenosis. However, although FFR is more suitable for assessing the functional significance of angiographically ambiguous lesions, OCT demonstrated a valuable complementary role in identifying the culprit sites and presence of potentially unstable lesions in cases with ACS and an FFR > 0.8.[21]

OCT USE DURING PCI PROCEDURES

Safety

The introduction of Fourier (or frequency)-domain OCT (FD-OCT), with more A-lines per frame, faster frame rates, and faster pullback speeds, enabled quicker image acquisition (a scan of 54 mm takes < 3 seconds) without the need of coronary blood flow occlusion. These characteristics made OCT procedures simpler, faster, and safer than the first-generation time-domain OCT, particularly with fewer complications, such as chest discomfort, transient arrhythmias, and electrocardiographic changes, increasing the interest for clinical application of OCT.[22,23] In fact, use of FD-OCT for PCI guidance was associated with a favorable safety profile.[24] In a large series of 297 FD-OCT acquisitions performed in 155 vessels in 150 all-comers patients, no procedure-related adverse events were recorded.[25]

Selection of PCI Strategy

Before PCI, OCT provides valuable information about plaque composition and extension, which may help in planning and guiding the interventional procedure and the use of adjunctive therapies. In cases of heavy calcification, OCT can accurately assess calcium circumferential extension and distance from the lumen,[26] contributing to decisions on avoiding direct stenting, performing lesion predilatation, and the use of adjunctive devices such as scoring balloons and rotational atherectomy.[27] Plaque composition at stent edges has been associated

with the occurrence of stent-edge dissections.[28] Avoiding stent placement over calcified or lipid-rich plaques might potentially reduce the occurrence of stent-edge dissections. Furthermore, placing stents over thin-capped fibroatheromas has been independently associated with the occurrence of periprocedural myocardial infarction (MI),[29] and possible disruption of such areas may lead to increased risk of late stent thrombosis (LST), as suggested by pathologic studies.[30]

OCT can also help to identify suitable normal (or "less diseased") vessel references for stent placement—the so-called stent landing zone. Because of limited tissue penetration, the adventitia is not always visualized, and quantification of the plaque burden is not an available option. Therefore, determination of stenosis severity and lesion length relies entirely upon proper lumen identification and may be cumbersome for less-experienced operators. Sites with the largest lumen proximal and distal to a stenosis and in the same arterial segment (usually within 10 mm of the stenosis with no major intervening side branches) have been used to define the proximal and distal references of a stenosis (Figure 2).[31] Importantly, this is not necessarily the site with the least amount of plaque. Accurate quantification of vascular lumen dimensions can also optimize the selection of balloon and stent sizes.

Assessment of Stent Expansion, Apposition, and Sizing

Stent underexpansion and malapposition have been linked to DES restenosis[32,33] and acute/subacute thrombosis.[34] To date, the use of intravascular imaging to define stent and/or balloon sizing has relied on distal vessel reference or average reference vessel sizes. Likewise, stent expansion is usually assessed by comparison of the minimum in-stent cross-section area (frequently by using single cross-section information to represent the

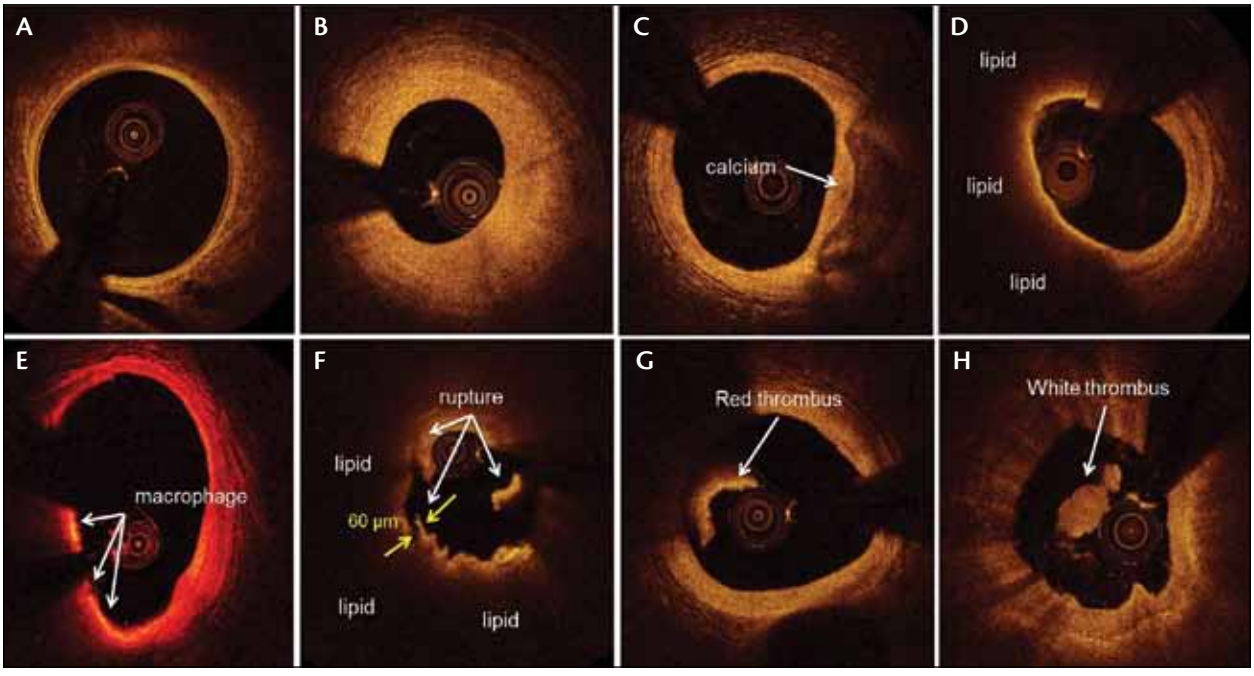

Figure 1. Characterization of atherosclerosis and plaque morphology by OCT. A normal vessel characterized by a three-layered architecture, comprising a highly backscattering or signal-rich intima, a low backscattering (low-intensity signal) media, and a highly backscattering adventitia (A). Fibrotic plaque with homogenous, high-backscattering OCT signal (B). Fibrocalcific plaque containing calcification characterized by a signal-poor or heterogeneous region, with sharply delineated borders (C). Thin-cap fibroatheroma composed of lipid pool/necrotic core defined as a signal-poor region with fast OCT signal drop-off and poorly delineated borders covered by a fibrous cap characterized as a signal-rich tissue layer overlying the signal-poor region. The fibrous cap thickness measured 50 µm (D).[1-3] Enhanced OCT cross-section image demonstrating macrophage accumulation within the fibrous cap, overlying a lipid-rich plaque; macrophage accumulation appears as confluent or punctuates highly backscattering focal regions within the artery wall (E).[6,7,29] Plaque rupture[8,29] as demonstrated by multiple tearing of a thin-cap fibroatheroma (lipid-rich plaque with fibrous cap thickness < 65 µm) (F). Thrombus characterized as a mass attached to the lumen surface or floating within the lumen (G, H). Red thrombus (red-cell rich thrombus): highly backscattering surface with high OCT signal attenuation (G). White thrombus: high, homogeneous backscattering with low OCT signal attenuation (H).[9]

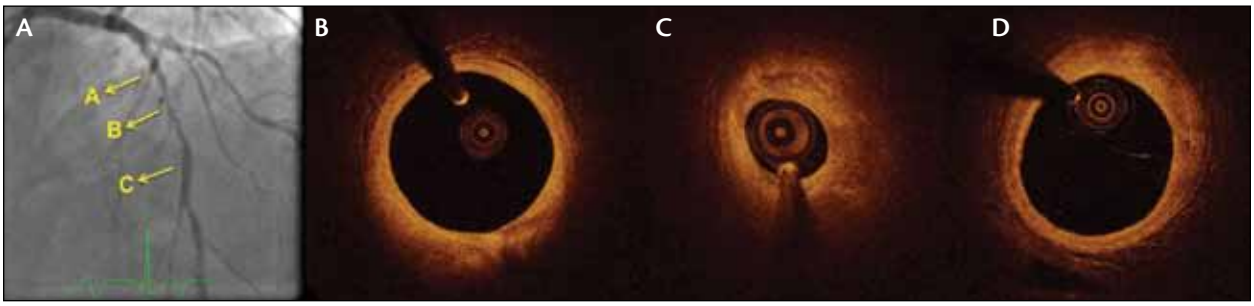

Figure 2. LAD angiography showing a severe diffuse lesion at the mid-portion (A). OCT cross-section images corresponding to proximal reference (B), with a maximum lumen diameter of 3.2 mm, minimum lumen area of 1 mm^2 (C), and distal reference with maximum lumen diameter of 2.9 mm (D).

whole stented segment) against predefined reference areas, which can be the proximal, distal, largest, or average reference area.[35] Current semiautomatic algorithms can easily and reproducibly quantify lumen and stent dimensions during OCT procedures in the catheterization laboratory, allowing quick recognition of minimal stent area and the estimation of stent expansion against the vascular references.

Stent strut apposition is part of most IVUS-guided PCI criteria for optimal stent implantation. Due to its high resolution, OCT is more sensitive than IVUS in detecting incomplete stent apposition (ISA), tissue prolapse, and in-stent thrombus formation.[36] Although acute ISA in the modern PCI era has not been associated with an increased occurrence of late adverse events,[37-39] it has been related to delayed vascular healing and incomplete endothelialization of stent struts at follow-up[40,41]—one of the most powerful pathological predictors for stent thrombosis.[30,42] The clinical and prognostic impact of frequent and usually small-sized stent malapposition as seen by OCT has yet to be defined. In a recent study, acute ISA size was an independent predictor of persistent ISA and grossly delayed coverage after 6-month follow-up.[43]

Assessing Acute Effects of PCI

Coronary stenting promotes differing degrees of vessel injury. Pathologic studies have indicated the association of implantation characteristics with late events after stent implantation.[44] Furthermore, IVUS studies have demonstrated that stent expansion, tissue protrusion, and edge dissections are associated with increased rates of early stent thrombosis.[39,45] Due to its high resolution, OCT can accurately assess the acute vascular response after coronary stent implantation (Figure 3). In a study of 80 vessels in 73 patients, OCT allowed a detailed visualization of vessel injury after stent implantation. Tissue prolapse within the stented segment was present in nearly all patients (97.5%) after stenting. In-stent dissections are also very frequent (86.3%), whereas stent-edge dissections were identified in 25% of the cases. A detailed quantification of the morphometric characteristics of such findings was also possible by OCT.[46] Still, because of its higher resolution, OCT clearly allows a much more detailed and frequent visualization of such phenomenon than IVUS, but the clinical impact of these findings is yet to be determined.

OCT-Guided PCI

To date, there are no randomized, prospective studies assessing the role of OCT-guided PCI. In a small study, OCT was performed after stent implantation in 74 patients to assess the need for further intervention. In 24 patients (32.4%), additional interventions were performed based on the OCT findings (15 patients underwent additional balloon dilatation, and nine patients underwent additional stenting). In the remaining 50 patients, the PCI results were deemed satisfactory, and no further interventions were performed, resulting in a 6-month event-free survival rate of 98%.[24]

Stefano et al[25] reported a series including unrestricted use of OCT in 150 consecutive patients (155 vessels) for pre-PCI evaluation or poststenting optimization. In this series, pre-PCI OCT imaging prompted changes in the initial angiography-based PCI strategy in 81.8% of the cases. Almost half of the angiographically planned stent lengths, one-quarter of stent diameters, and more than half of the postdilatation balloon diameters were altered based on OCT imaging. The use of OCT after PCI led to further interventions in 54.8% of the target vessels, mostly by inducing additional balloon dilatations to correct stent malappositions or implanting additional stents to treat edge dissections.

In the study by Viceconte et al,[47] OCT was used to guide coronary stenting in 108 patients. Sixty-eight OCT pullbacks were performed before PCI, leading to deferral of the procedure in 13 (19.1%) and use of adjunctive

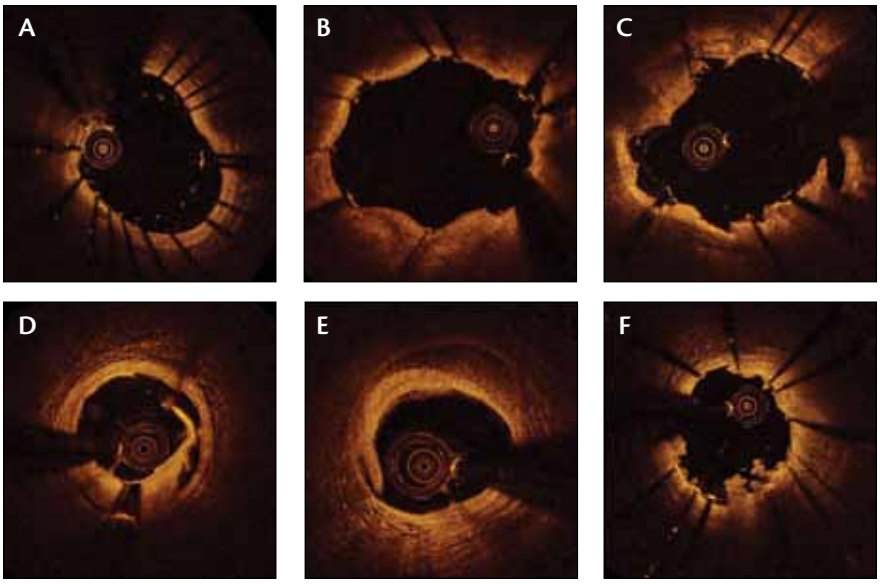

Figure 3. Acute effects of PCI as assessed by OCT. Stent malapposition showing separation of stent struts from the vessel wall in which the distance between the strut's surface to the luminal surface is greater than the strut thickness (including polymer, if present) (A).[29] Plaque prolapse defined as projection of tissue into the lumen between stent struts after its implantation without disruption of the continuity of the lumen surface (B).[29,44] In-stent dissection characterized as disruption of the luminal vessel surface within the stented segment (C).[44] Stent edge dissection characterized by disruption of the luminal surface continuity at either the proximal or distal edge outside the stent (D).[29,44] Intramural hematoma defined as an accumulation of blood (or flushing media) within the medial space, displacing the internal elastic membrane inward and the external elastic membrane outward (E).[29] In-stent thrombus characterized by irregular mass protruding into the lumen, between or on top of the stent struts, with or without dorsal attenuation (F).[29,44]

devices in 23 (33.8%). Out of 207 pullbacks performed after stenting, 29 (14%) led to additional stent implantation either because of edge dissection or residual stenosis, and further stent optimization with a high-pressure/larger-sized balloon was suggested in 64 (30.9%). In another small case series study, OCT measurements safely allowed upsizing of the cutting balloon, resulting in an acceptable lumen increase before deployment of another DES for in-stent restenosis.[48]

Lastly, Prati et al[49] compared the 1-year clinical outcomes of 335 patients undergoing PCI with angiographic plus OCT guidance against a matched group of another 335 patients undergoing PCI with angiographic guidance alone. Per protocol, some recommendations were advised when signs of acute vascular injury were detected by OCT: (1) edge dissections and reference lumen narrowing had to be treated with an additional stent; (2) stent underexpansion (in-stent MLA ≥ 90% of the average reference lumen area or ≥ 100% of lumen area of the reference segment with the lowest lumen area) required further dilatation of the implanted stent with a noncompliant balloon of the same size at ≥ 18 atm or with a semicompliant balloon having a diameter ≥ 0.25 mm larger than the previously used balloon at ≥ 14 atm; (3) stent malapposition required further dilatation of the implanted stent with a noncompliant or semicompliant balloon having a diameter ≥ 0.25 mm larger than the previously used balloon at ≥ 14 atm; and (4) intraluminal thrombus required further dilatation of the stent with a noncompliant or semicompliant balloon of the same diameter at 8 to 14 atm for 60 seconds. OCT discovered adverse features requiring interventions in 34.7% of the cases. Unadjusted analysis revealed that the OCT group had a significantly lower 1-year risk of cardiac death (1.2% vs 4.5%; *P* = .01), cardiac death or MI (6.6% vs 13%; *P* = .006), and the composite of cardiac death, MI, or repeat revascularization (9.6% vs 14.8%; *P* = .044). After extensive adjustments by multivariate analysis and propensity score–adjusted analysis, angiographic plus OCT guidance was still associated with a significantly lower risk of cardiac death or MI (odds ratio, 0.49; 95% confidence interval, 0.25–0.96; *P* = .037).

Despite these favorable results, the magnitude of OCT-detected vascular injury that deserves further interventions is still controversial. Whether OCT-guided stent optimization will lead to improved clinical outcomes in the contemporary era of new-generation DES and potent adjunct pharmacology has yet to be determined in large, prospective, randomized trials.

ASSESSMENT OF LONG-TERM RESULTS AFTER PCI

The extent of endothelialization has been suggested by pathologic studies as one of the strongest predictors for late DES thrombosis, hence introducing the need for detailed, in vivo assessment of stent strut coverage. For many years, IVUS has been considered the gold standard imaging modality to assess long-term results of coronary

stenting. Although IVUS was the standard tool for neointimal hyperplasia quantification at follow-up, it lacks the axial resolution to resolve the thin neointimal coverage in the DES era, when the average late loss of modern second-generation DES is as low as 0.1 to 0.2 mm. OCT has 10-fold greater resolution than IVUS and demonstrated a high correlation with histology for the evaluation of neointimal area and neointimal thickness,[50,51] providing detailed in vivo assessment of stent coverage as a surrogate marker for stent safety.[52] Nevertheless, the correlation of OCT evaluation of stent coverage and late adverse clinical events has yet to be determined.

A recent study by Guagliumi et al[53] was the first attempt to investigate, in vivo, the role of uncovered struts in patients with definite LST after DES implantation. In this study, 18 patients experiencing DES LST (median, 615 days after implantation) undergoing emergent PCI were compared with 36 matched DES control subjects undergoing routine repeat OCT and IVUS who did not experience LST for a period of ≥ 3 years. By OCT, patients with LST had a higher percentage of uncovered (median [interquartile range]; 12.27 [5.5–23.33] vs 4.14 [3–6.22]; $P < .001$) and malapposed struts (4.6 [1.85–7.19] vs 1.81 [0–2.99]; $P < .001$) in comparison to the control group. By IVUS, positive vascular remodeling was increased in patients with LST (mean vessel cross-section area, 19.4 ± 5.8 mm^2 vs 15.1 ± 4.6 mm^2; $P = .003$). By multivariate analysis, the length of segments with uncovered stent struts by OCT and the remodeling index by IVUS were independent predictors of LST.

OCT can also be used for elucidating other mechanisms of late stent failures. Different patterns of neointimal hyperplasia can be easily characterized by OCT,[54,55] allowing for the identification of areas consistent with the presence of peristrut fibrinoid and proteoglycan deposition,[56] as well as the occurrence of in-stent neoatherosclerosis (Figure 4),[57,58] which has been recently linked to late restenosis and LST.[58-62]

Furthermore, although IVUS is more sensitive in detecting stent fracture than angiography,[63] limited resolution along with the frequent occurrence of acoustic and heart motion artifacts may affect its ability to detect small strut fractures. By providing fewer artifacts, faster pullback speeds, and higher axial resolution, intravascular OCT can be an important adjunctive tool for the clinical diagnosis of this complication.[64-66] Moreover, investigation of structural integrity is of particular importance for the acute and late success of new polymeric bioresorbable scaffold technologies.

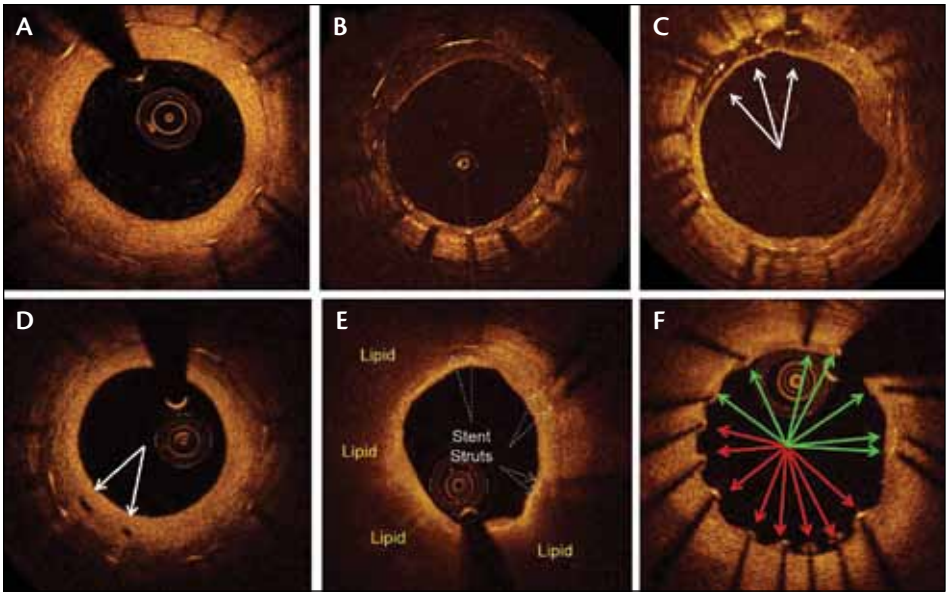

Figure 4. Different patterns of vascular healing following stent implantation. Homogeneous, highly backscattering (high OCT signal intensity) neointimal hyperplastic tissue (A). Heterogeneous neointimal hyperplastic tissue with predominantly low backscattering (low OCT signal intensity) (B). Peristrut infiltrate defined as a homogeneous region around stent struts with lower optical signal intensity than the surrounding tissues, without significant dorsal attenuation (C).[54] Microvessels within the neointimal tissue characterized by well-delineated low-backscattering structures < 200 µm in diameter that show a trajectory within the vessel (D).[52] Lipid-laden neointima characterized by abrupt reduction in the optical signal with diffuse boundaries, with an overlying high-backscattering fibrous cap (similar to lipid plaques in nonstented vessels) (E).[55,56] Heterogeneous strut coverage with the presence of covered (green arrows) and uncovered (red arrows) struts in the same OCT cross-section image (F).

PERSPECTIVES FOR THE FUTURE

A great amount of effort has been dedicated toward automating the segmentation process of acquired OCT images. Automatic lumen segmentation will provide operators with a fast and accurate quantification of vascular dimensions, making it very easy and intuitive to estimate the degree of lesion stenosis and select the size of intracoronary stents. Algorithms enabling automated tissue characterization will allow for a more objective assessment

of plaque morphology and composition.[67,68] The same is true for automated stent strut detection and segmentation algorithms,[69] which will provide fast quantification of stent dimensions and identification of sites of stent underexpansion and malapposition.

Three-dimensional volumetric OCT datasets are capable of providing a large amount of data in a very intuitive and comprehensive way, aiding the interpretation and analysis of atherosclerosis and vessel/stent interaction.[70,71] Automation of lumen and stent segmentation will serve as the basis for faster three-dimensional OCT reconstruction software, available online in the cath lab, with the potential to add information regarding vascular and stent geometries, as well as stent expansion and its relation to surrounding structures. Algorithms providing fusion of intravascular OCT images and angiography carry the potential to improve the interpretation of coronary artery disease and the guidance of coronary intervention.[72,73]

Despite all the potential for clinical use of OCT images, there are still no clear indications for the clinical application of OCT. Ongoing and future studies validating the clinical use of OCT in all-comers and selected population subgroups will determine the role of OCT in procedural guidance.

CONCLUSION

OCT is a recently introduced high-resolution imaging modality with unique features that provide detailed information regarding the vascular biology. OCT has established itself in the research scenario as an invaluable tool for atherosclerosis characterization, especially in the detection of vulnerable plaques, and assessment of vascular response to intracoronary devices. The large amount of detailed structural information along with great potential for technology and software development makes OCT a promising intravascular tool for clinical decision making and guiding and optimizing interventional procedures. Whether these beneficial advantages will translate to an improvement in patient-related outcomes is an issue to be determined in large prospective studies and registries. ■

Daniel Chamié, MD, is with the Department of Invasive Cardiology, Instituto Dante Pazzanese de Cardiologia in São Paulo, Brazil. He has disclosed that he has no financial interests related to this article.

Ricardo A. Costa, MD, PhD, is with the Department of Invasive Cardiology, Instituto Dante Pazzanese de Cardiologia in São Paulo, Brazil. He has disclosed that he has no financial interests related to this article. Dr. Costa may be reached at +55 (11) 5085-6000; rcosta@dantepazzanese.org.br.

1. Tanigawa J, Barlis P, Di Mario C. Intravascular optical coherence tomography: optimisation of image acquisition and quantitative assessment of stent strut apposition. EuroIntervention. 2007;3:128-136.
2. Bezerra HG, Costa MA, Guagliumi G, et al. Intracoronary optical coherence tomography: a comprehensive review clinical and research applications. JACC Cardiovasc Interv. 2009;2:1035-1046.
3. Yabushita H, Bouma BE, Houser SL, et al. Characterization of human atherosclerosis by optical coherence tomography. Circulation. 2002;106:1640-1645.
4. Kume T, Akasaka T, Kawamoto T, et al. Assessment of coronary intima--media thickness by optical coherence tomography: comparison with intravascular ultrasound. Circ J. 2005;69:903-907.
5. Jang IK, Bouma BE, Kang DH, et al. Visualization of coronary atherosclerotic plaques in patients using optical coherence tomography: comparison with intravascular ultrasound. JACC. 2002;39:604-609.
6. Cilingiroglu M, Oh JH, Sugunan B, et al. Detection of vulnerable plaque in a murine model of atherosclerosis with optical coherence tomography. Catheter Cardiovasc Interv. 2006;67:915-923.
7. Kume T, Akasaka T, Kawamoto T, et al. Measurement of the thickness of the fibrous cap by optical coherence tomography. Am Heart J. 2006;152:755;e751-754.
8. MacNeill BD, Jang IK, Bouma BE, et al. Focal and multi-focal plaque macrophage distributions in patients with acute and stable presentations of coronary artery disease. JACC. 2004;44:972-979.
9. Tearney GJ, Yabushita H, Houser S, et al. Quantification of macrophage content in atherosclerotic plaques by optical coherence tomography. Circulation. 2002;107:113-119.
10. Kubo T, Imanishi T, Takarada S, et al. Assessment of culprit lesion morphology in acute myocardial infarction: ability of optical coherence tomography compared with intravascular ultrasound and coronary angioscopy. JACC. 2007;50:933-939.
11. Kume T, Akasaka T, Kawamoto T, et al. Assessment of coronary arterial thrombus by optical coherence tomography. Am J Cardiol. 2006;97:1713-1717.
12. Tahara S, Bezerra HG, Baibars M, et al. In vitro validation of new fourier-domain optical coherence tomography. EuroIntervention. 2011;6:875-882.
13. Gonzalo N, Garcia-Garcia HM, Serruys PW, et al. Reproducibility of quantitative optical coherence tomography for stent analysis. EuroIntervention. 2009;5:224-232.
14. Tanimoto S, Rodriguez-Granillo G, Barlis P, et al. A novel approach for quantitative analysis of intracoronary optical coherence tomography: high inter-observer agreement with computer-assisted contour detection. Catheter Cardiovasc Interv. 2008;72:228-235.
15. Gonzalo N, Serruys PW, Garcia-Garcia HM, et al. Quantitative ex vivo and in vivo comparison of lumen dimensions measured by optical coherence tomography and intravascular ultrasound in human coronary arteries. Rev Esp Cardiol. 2009;62:615-624.
16. Abizaid A, Mintz GS, Pichard AD, et al. Clinical, intravascular ultrasound, and quantitative angiographic determinants of the coronary flow reserve before and after percutaneous transluminal coronary angioplasty. Am J Cardiol. 1998;82:423-428.
17. Briguori C, Anzuini A, Airoldi F, et al. Intravascular ultrasound criteria for the assessment of the functional significance of intermediate coronary artery stenoses and comparison with fractional flow reserve. Am J Cardiol. 2001;87:136-141.
18. Nishioka T, Amanullah AM, Luo H, et al. Clinical validation of intravascular ultrasound imaging for assessment of coronary stenosis severity: comparison with stress myocardial perfusion imaging. JACC. 1999;33:1870-1878.
19. Kang SJ, Lee JY, Ahn JM, et al. Intravascular ultrasound-derived predictors for fractional flow reserve in intermediate left main disease. JACC Cardiovasc Interv. 2011;4:1168-1174.
20. Gonzalo N, Escaned J, Alfonso F, et al. Morphometric assessment of coronary stenosis relevance with optical coherence tomography: a comparison with fractional flow reserve and intravascular ultrasound. JACC. 2012;59:1080-1089.
21. Stefano GT, Bezerra HG, Attizzani G, et al. Utilization of frequency domain optical coherence tomography and fractional flow reserve to assess intermediate coronary artery stenoses: conciliating anatomic and physiologic information. Int J Cardiovasc Imaging. 2011;27:299-308.
22. Okamura T, Onuma Y, Garcia-Garcia HM, et al. First-in-man evaluation of intravascular optical frequency domain imaging (OFDI) of terumo: a comparison with intravascular ultrasound and quantitative coronary angiography. EuroIntervention. 2011;6:1037-1045.
23. Takarada S, Imanishi T, Liu Y, et al. Advantage of next-generation frequency-domain optical coherence tomography compared with conventional time-domain system in the assessment of coronary lesion. Catheter Cardiovasc Interv. 2010;75:202-206.
24. Imola F, Mallus MT, Ramazzotti V, et al. Safety and feasibility of frequency domain optical coherence tomography to guide decision making in percutaneous coronary intervention. EuroIntervention. 2010;6:575-581.
25. Stefano GT, Bezerra HG, Mehanna E, et al. Unrestricted utilization of frequency domain optical coherence tomography in coronary interventions. Int J Cardiovasc Imaging. In press.
26. Kume T, Okura H, Kawamoto T, et al. Assessment of the coronary calcification by optical coherence tomography. EuroIntervention. 2011;6:768-772.
27. Attizzani GF, Patricio L, Bezerra HG. Optical coherence tomography assessment of calcified plaque modification after rotational atherectomy. Catheter Cardiovasc Interv. In press.
28. Gonzalo N, Serruys PW, Okamura T, et al. Relation between plaque type and dissections at the edges after stent implantation: an optical coherence tomography study. Int J Cardiol. 2011;150:151-155.
29. Porto I, Di Vito L, Burzotta F, et al. Predictors of periprocedural (type IVa) myocardial infarction, as assessed by frequency-domain optical coherence tomography. Circ Cardiovasc Interv. 2012;5:89-96;S81-86.
30. Joner M, Finn AV, Farb A, et al. Pathology of drug-eluting stents in humans: delayed healing and late thrombotic risk. JACC. 2006;48:193-202.
31. Tearney GJ, Regar E, Akasaka T, et al. Consensus standards for acquisition, measurement, and reporting of intravascular optical coherence tomography studies: a report from the international working group for intravascular optical coherence tomography standardization and validation. J Am Coll Cardiol. 2012;59:1058-1072.
32. Fujii K, Mintz GS, Kobayashi Y, et al. Contribution of stent underexpansion to recurrence after sirolimus-eluting stent implantation for in-stent restenosis. Circulation. 2004;109:1085-1088.
33. Hong MK, Mintz GS, Lee CW, et al. Intravascular ultrasound predictors of angiographic restenosis after sirolimus-eluting stent implantation. Eur Heart J. 2006;27:1305-1310.
34. Fujii K, Carlier SG, Mintz GS, et al. Stent underexpansion and residual reference segment stenosis are related to stent thrombosis after sirolimus-eluting stent implantation: an intravascular ultrasound study. J Am Coll Cardiol. 2005;45:995-998.
35. Mintz GS, Nissen SE, Anderson WD, et al. American college of cardiology clinical expert consensus document on standards for acquisition, measurement and reporting of intravascular ultrasound studies (IVUS). A report of the American College of Cardiology task force on clinical expert consensus documents. J Am Coll Cardiol. 2001;37:1478-1492.

36. Bouma BE, Tearney GJ, Yabushita H, et al. Evaluation of intracoronary stenting by intravascular optical coherence tomography. Heart. 2003;89:317-320.
37. Hoffmann R, Morice MC, Moses JW, et al. Impact of late incomplete stent apposition after sirolimus-eluting stent implantation on 4-year clinical events: intravascular ultrasound analysis from the multicentre, randomised, RAVEL, E-SIRIUS and SIRIUS trials. Heart. 2008;94:322-328.
38. Steinberg DH, Mintz GS, Mandinov L, et al. Long-term impact of routinely detected early and late incomplete stent apposition: an integrated intravascular ultrasound analysis of the TAXUS IV, V, and VI and TAXUS ATLAS WORKHORSE, LONG LESION, and DIRECT STENT studies. JACC Cardiovasc Interv. 2010;3:486-494.
39. Choi SY, Witzenbichler B, Maehara A, et al. Intravascular ultrasound findings of early stent thrombosis after primary percutaneous intervention in acute myocardial infarction: a harmonizing outcomes with revascularization and stents in acute myocardial infarction (HORIZONS-AMI) substudy. Circ Cardiovasc Interv. 2011;4:239-247.
40. Radu M, Jorgensen E, Kelbaek H, et al. Optical coherence tomography at follow-up after percutaneous coronary intervention: relationship between procedural dissections, stent strut malapposition and stent healing. EuroIntervention. 2011;7:353-361.
41. Gutierrez-Chico JL, Regar E, Nuesch E, et al. Delayed coverage in malapposed and side-branch struts with respect to well-apposed struts in drug-eluting stents: in vivo assessment with optical coherence tomography. Circulation. 2011;124:612-623.
42. Finn AV, Joner M, Nakazawa G, et al. Pathological correlates of late drug-eluting stent thrombosis: strut coverage as a marker of endothelialization. Circulation. 2007;115:2435-2441.
43. Gutierrez-Chico JL, Wykrzykowska J, Nuesch E, et al. Vascular tissue reaction to acute malapposition in human coronary arteries: sequential assessment with optical coherence tomography. Circ Cardiovasc Interv. 2012;5:20-29, S21-28.
44. Farb A, Burke AP, Kolodgie FD, Virmani R. Pathological mechanisms of fatal late coronary stent thrombosis in humans. Circulation. 2003;108:1701-1706.
45. Liu X, Doi H, Maehara A, et al. A volumetric intravascular ultrasound comparison of early drug-eluting stent thrombosis versus restenosis. JACC Cardiovasc Interv. 2009;2:428-434.
46. Gonzalo N, Serruys PW, Okamura T, et al. Optical coherence tomography assessment of the acute effects of stent implantation on the vessel wall: a systematic quantitative approach. Heart. 2009;95:1913-1919.
47. Viceconte N, Chan PH, Barrero EA, et al. Frequency domain optical coherence tomography for guidance of coronary stenting. Int J Cardiol. In press.
48. Secco GG, Foin N, Viceconte N, et al. Optical coherence tomography for guidance of treatment of in-stent restenosis with cutting balloons. EuroIntervention. 2011;7:828-834.
49. Prati F, Di Vito L, Biondi-Zoccai G, et al. Angiography alone versus angiography plus optical coherence tomography to guide decision-making during percutaneous coronary intervention: the centro per la lotta contro l'infarto-optimisation of percutaneous coronary intervention (CLI-OPCI) study. EuroIntervention. 2012;8:823-829.
50. Murata A, Wallace-Bradley D, Tellez A, et al. Accuracy of optical coherence tomography in the evaluation of neointimal coverage after stent implantation. JACC Cardiovasc Imaging. 2010;3:76-84.
51. Templin C, Meyer M, Muller MF, et al. Coronary optical frequency domain imaging (OFDI) for in vivo evaluation of stent healing: comparison with light and electron microscopy. Eur Heart J. 2010;31:1792-1801.
52. Tahara S, Chamie D, Baibars M, et al. Optical coherence tomography endpoints in stent clinical investigations: strut coverage. Int J Cardiovasc Imaging. 2011;27:271-287.
53. Guagliumi G, Sirbu V, Musumeci G, et al. Examination of the in vivo mechanisms of late drug-eluting stent thrombosis: findings from optical coherence tomography and intravascular ultrasound imaging. JACC Cardiovasc Interv. 2012;5:12-20.
54. Gonzalo N, Serruys PW, Okamura T, et al. Optical coherence tomography patterns of stent restenosis. Am Heart J. 2009;158:284-293.
55. Habara M, Terashima M, Nasu K, et al. Difference of tissue characteristics between early and very late restenosis lesions after bare-metal stent implantation: an optical coherence tomography study. Circ Cardiovasc Interv. 2011;4:232-238.
56. Teramoto T, Ikeno F, Otake H, et al. Intriguing peri-strut low-intensity area detected by optical coherence tomography after coronary stent deployment. Circ J. 2010;74:1257-1259.
57. Hou J, Qi H, Zhang M, et al. Development of lipid-rich plaque inside bare metal stent: possible mechanism of late stent thrombosis? An optical coherence tomography study. Heart. 2010;96:1187-1190.
58. Kang SJ, Mintz GS, Akasaka T, et al. Optical coherence tomographic analysis of in-stent neoatherosclerosis after drug-eluting stent implantation. Circulation. 2011;123:2954-2963.
59. Bennett J, Coosemans M, Adriaenssens T. Very late bare metal stent thrombosis due to neoatherosclerotic plaque rupture: an optical coherence tomography finding. Heart. 2012;98:1470.
60. Koga S, Ikeda S, Yoshida T, et al. Very late stent thrombosis caused by rupture of lipid-laden neointima in a self-expanding coronary stent. Int Heart J. 2012;53:202-204.
61. Ko YG, Kim DM, Cho JM, et al. Optical coherence tomography findings of very late stent thrombosis after drug-eluting stent implantation. Int J Cardiovasc Imaging. 2012;28:715-723.
62. Ando H, Ishii H, Yoshikawa D, et al. Disruption of atherosclerotic neointima as a cause of very late stent thrombosis after bare metal stent implantation. Am J Cardiol. 2012;109:448-449.
63. Yamada KP, Koizumi T, Yamaguchi H, et al. Serial angiographic and intravascular ultrasound analysis of late stent strut fracture of sirolimus-eluting stents in native coronary arteries. Int J Cardiol. 2008;130:255-259.
64. Barlis P, Sianos G, Ferrante G, et al. The use of intra-coronary optical coherence tomography for the assessment of sirolimus-eluting stent fracture. Int J Cardiol. 2009;136:e16-20.
65. Nakano M, Vorpahl M, Otsuka F, Virmani R. Optical frequency domain imaging of stent fracture and coronary dissection associated with intraplaque hemorrhage. JACC Cardiovasc Interv. 2011;4:1047-1048.
66. Okamura T, Matsuzaki M. Sirolimus-eluting stent fracture detection by three-dimensional optical coherence tomography. Catheter Cardiovasc Interv. 2012;79:628-632.
67. van Soest G, Goderie T, Regar E, et al. Atherosclerotic tissue characterization in vivo by optical coherence tomography attenuation imaging. J Biomed Opt. 2010;15:011105.
68. Wang Z, Kyono H, Bezerra HG, et al. Semiautomatic segmentation and quantification of calcified plaques in intracoronary optical coherence tomography images. J Biomed Opt. 2010;15:061711.
69. Unal G, Gurmeric S, Carlier SG. Stent implant follow-up in intravascular optical coherence tomography images. Int J Cardiovasc Imaging. 2010;26:809-816.
70. Chamié D, Prabhu D, Wang Z, et al. Three-dimensional fourier-domain optical coherence tomography imaging: advantages and future development. Curr Cardiovasc Imaging Rep. 2012;5:221-230.
71. Farooq V, Okamura T, Gogas BD, et al. 3D reconstructions of optical frequency domain imaging to improve understanding of conventional pci. JACC Cardiovasc Imaging. 2011;4:1044-1046.
72. Tu S, Holm NR, Koning G, et al. Fusion of 3D QCA and IVUS/OCT. Int J Cardiovasc Imaging. 2011;27:197-207.
73. Bourantas CV, Papafaklis MI, Naka KK, et al. Fusion of optical coherence tomography and coronary angiography—in vivo assessment of shear stress in plaque rupture. Int J Cardiol. 2012;155:e24-26.